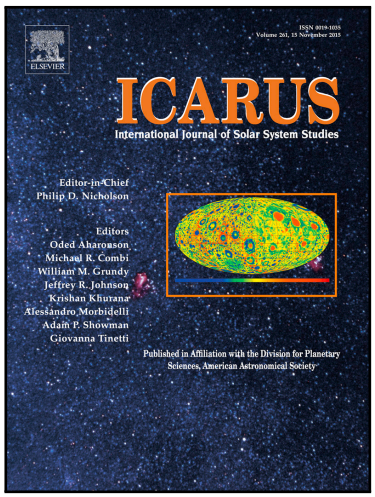

Occator Crater in Color at Highest Spatial Resolution

A. Nathues , T. Platz , G. Thangjam , M. Hoffmann , J.E.C. Scully , N. Stein , O. Ruesch , K. Mengel

PII: S0019-1035(17)30639-5
DOI: 10.1016/j.icarus.2017.12.021
Reference: YICAR 12741

To appear in: *Icarus*

Received date: 5 September 2017
Revised date: 22 November 2017
Accepted date: 12 December 2017

Please cite this article as: A. Nathues , T. Platz , G. Thangjam , M. Hoffmann , J.E.C. Scully , N. Stein , O. Ruesch , K. Mengel , Occator Crater in Color at Highest Spatial Resolution, *Icarus* (2017), doi: 10.1016/j.icarus.2017.12.021

Highlights

- Brines from reservoir(s) at depth extruded onto the floor of Occator crater.
- The youngest deposition is less than about 2 Ma old.
- Faculae material is fed trough fractures and vents.
- Distribution and thickness of sub-surface brine layers is inhomogeneous.
- Updoming is present on the southwestern crater floor.

Occator Crater in Color at Highest Spatial Resolution

Nathues, A.[1], Platz, T.[1], Thangjam, G.[1], Hoffmann, M.[1], Scully J. E. C.[2], Stein, N.[3], Ruesch, O.[4], and Mengel K[5].

[1]Max Planck Institute for Solar System Research, Justus-von-Liebig-Weg 3, 37077 Goettingen, Germany (nathues@mps.mpg.de),

[2]Jet Propulsion Laboratory, California Institute of Technology, 4800 Oak Grove Drive, Pasadena, CA 91109

[3]Division of Geological and Planetary Sciences, California Institute of Technology, Pasadena, CA, 91125.

[4] NASA Goddard Space Flight Center/USRA, Greenbelt, MD 20771, USA.

[5]IELF, TU Clausthal, Adolph-Roemer-Straße 2A, 38678 Clausthal-Zellerfeld, Germany

Pages: 40

Figures: 15

Tables: 0

Keywords: Asteroid Ceres, Asteroids, composition, surfaces, Mineralogy, Spectroscopy

Proposed Running Head: Occator in colors

***Editorial correspondence to:**

Andreas Nathues
Max-Planck Institute for Solar System Research,
Justus-von-Liebig-Weg 3,
37077 Göttingen,
Germany
nathues@mps.mpg.de
Tel.: +49 551 384 979 433

ABSTRACT

The geology of the outstanding crater Occator on Ceres has been studied by combining highest resolution color images and other information from the DAWN mission. Thus**,** surface and sub-surface layers and **geologic** processes can be understood and interpreted in a consistent manner. In order to achieve this, morphometry, **absolute** surface unit ages, color, and the distribution of foci of activity were the key data. **These data** show that the ascent of brine from reservoir(s) at depth and deposition of its salts on the surface persisted much longer than initially thought possible as an immediate result of the primary impact. The youngest depositional processes of bright material occurred less than 2 Ma ago. Also, the bright Cerealia and Vinalia faculae are not the only traces of this activity; updoming is present on the southwestern crater floor. Faculae coincide with fractures and vents and indicate complex mechanisms of the deposition of bright carbonate-rich material. Due to the large age difference between the Occator impact itself, modeled cooling times of heated crater material, and the recent activity at the faculae we conclude that endogenic forces were lately acting. The distribution and thickness of surface and sub-surface brine layers are far from homogeneous in the upper crust beneath Occator. Further evidence regarding the distribution of materials has been derived from the distribution of the ejecta and the transition of ejecta to background material outside the crater.

1. INTRODUCTION

The Framing Cameras (FCs) FC1 and FC2 are payloads of the Dawn spacecraft (Russell and Raymond 2012). To date (August 2017) camera FC2 has obtained ~57,000 images of Ceres in seven spectral bands (0.44 - 0.98 µm) and one panchromatic filter (Sierks et al. 2012), performing global color mapping of the surface of Ceres at a resolution of ~140 m/pixel (Russell et al. 2016, Nathues et al. 2016; Fig. 1). In addition, color data with a resolution of ~35 m/pixel have been obtained for a number of selected sites (Nathues et al. 2017a, b). One of the prime targets was the crater Occator, hosting the brightest surface features on Ceres (Nathues et al. 2015a, Nathues et al. 2016, Nathues et al. 2017a, Ruesch et al. this issue, Stein et al. this issue, Quick et al., this issue). These bright features have been commonly referred to as 'bright spots' and have been named Cerealia Facula (central bright spot) and Vinalia Faculae (secondary bright spots) (Figs 2 and 3). The bright spots populate a portion of the floor of Occator that shows evidence of a diurnal brightness variation, which was attributed to local haze (Nathues et al. 2015a, Thangjam et al. 2016). Spectral analysis of Dawn's Visible and Infrared Spectrometer (VIR) data revealed that these bright spots are dominated by sodium carbonate mixed with some dark ammoniated minerals (De Sanctis et al. 2016). De Sanctis et al. 2016 also concluded that carbonates and ammoniated minerals are present on Occator's floor as well as on a global scale. Nathues et al. (2017a) reported that the surface of Cerealia Facula is about 30 Myr younger than the Occator crater itself, which formed at about 34 Ma. Cerealia Facula comprises a central pit whose center exhibits a dome that is spectrally rather homogenous, exhibiting absorption features that are consistent with carbonates (**De Sanctis et al. 2016,** Nathues et al. 2017a). The dome is likely the outcome of a long lasting, periodic or episodic ascent of bright material from a subsurface brine reservoir enriched primarily in carbonates **(Nathues et al. 2017a)**. Originally

triggered by an impact event, gases, possibly exsolved from a subsurface brine reservoir, enabled this material to ascend through fractures and be deposited onto the surface (Nathues et al. 2017a, Ruesch et al. this issue, Stein et al. this issue).

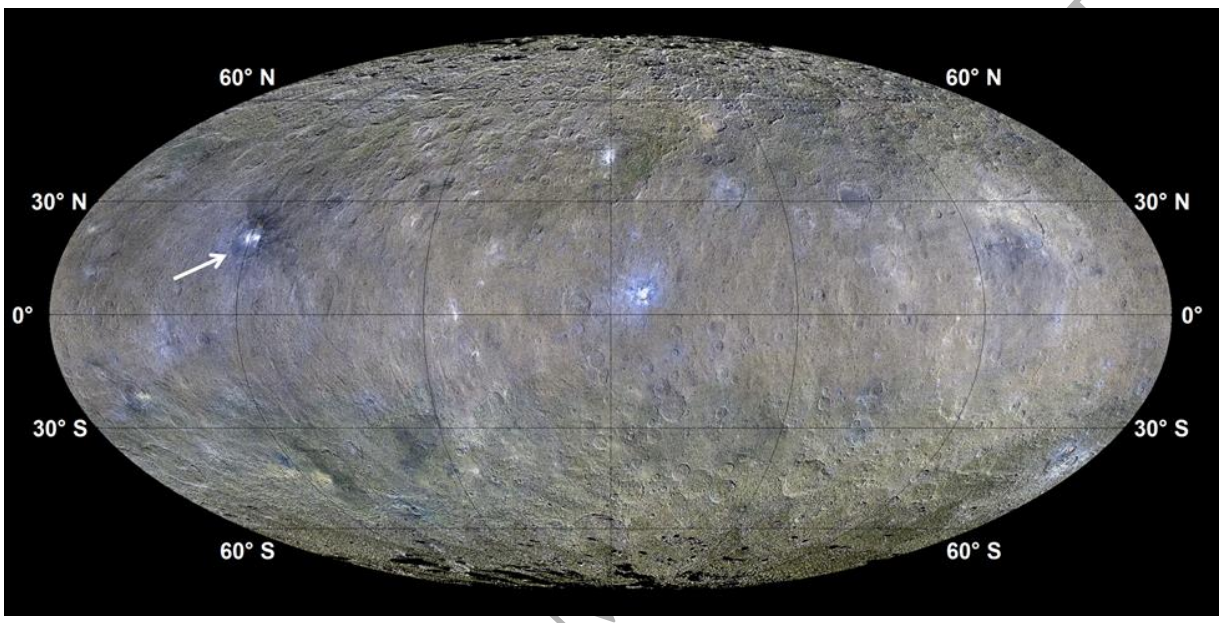

Fig. 1: Enhanced global color mosaic of the surface of Ceres. Data have been obtained at a resolution of ~140 m/pixel from HAMO and XMO2 orbits. A white arrow marks the location of the Occator crater showing the brightest surface feature on Ceres. RGB colors are R = 0.96 µm, G = 0.65 µm, and B = 0.44 µm ***(red range: 0.022-0.039, green range: 0.023-0.042, blue range: 0.022-0.038)****. Mollweide projection centered at the prime meridian; longitudinal graticule is in 30° increments. Modified after Nathues et al. (2017b).*

The surface of Ceres is peppered with hundreds of bright, carbonate-bearing areally small spots, which are less bright than those present at Occator (Nathues et al. 2015a: extended data Fig. 1, Nathues et al. 2016, Nathues et al. 2017b, Stein et al. this issue, Palomba et al. this issue, Thangjam et al. **in review**). Because Cerealia and Vinalia faculae are the brightest and likely

youngest spots on the surface, Occator provides a case to understand the processes that formed and modified the other bright spots. Beside Occator, smaller bright spots were identified on the floors of seven further large, deep, and fresh to moderately degraded impact craters (Stein et al. this issue). The morphology of these bright spots and the surrounding crater floor is consistent with impact-induced heating and upwelling of volatile-rich material. Small bright spots prevalent on crater rims and ejecta were found to occur in and around hundreds of relatively young craters of all sizes consistent with the excavation of bright material that was previously emplaced, either by past impact processes or by heterogeneously distributed subsurface processes (Stein et al., this issue). It was also found that bright spots darken over time primarily due to impact-induced mixing with dark material (Nathues et al. 2017a, Palomba et al this issue). Stein et al. (this issue) estimate that on average, bright spots are buried by impact-induced mixing or directly disseminated by impacts over periods of less than 1 Gyr.

Some of the carbonate-bearing bright areas contain significant amounts of water ice **which was most recently** excavated **by material slumping in fresh** impact craters (Nathues et al. 2015, Combe et al. 2016, Nathues et al. 2017b, Combe et al. in review). **In addition, an ice layer was build up by cold-trapping** of water molecules in **some** northern shadowed regions (Platz et al. 2016, Schorghofer et al. 2016).

In this study we report our continued analyses of the evolution of Occator crater based on FC color imagery at the highest spatial resolution (~35 m/pixel) leading to further insights of how Occator crater evolved. We also report on the morphometry of Occator crater based on the highest-resolution digital terrain model and characterize the extent of its ejecta blanket as seen in FC clear filter and color images.

2. DATA PROCESSING AND METHOD

The Framing Camera FC2 onboard Dawn has imaged the entire illuminated surface of (1) Ceres since March 2015. Ceres was mapped from Survey, HAMO (High-Altitude Mapping Orbit) and LAMO (Low-Altitude Mapping Orbit) at spatial resolutions of ~400 m/pixel, ~140 m/pixel, and ~35 m/pixel, respectively. During the extended mission phase a number of higher orbits have been flown, from which we use data of the XMO2 orbit (Extended Mission Orbit 2; ~140 m/pixel). This orbit was used to increase the illuminated surface coverage of the south polar region as Ceres moved closer to the ascending node.

FC color images exist in three standard levels: 1a, 1b, and 1c (color only), from which we used level 1b (clear filter) and 1c (colors)—details are described in Nathues et al. (2014, 2015b). Level 1b/c data are converted to reflectance (I/F) by dividing the observed radiance by solar irradiance from a normally solar-illuminated Lambertian disk. Color cubes are derived by applying an in-house image processing pipeline as described in Reddy et al. (2012) and Nathues et al. (2014, 2015b). Color cubes are photometrically corrected to standard viewing geometry (i.e., 30° phase**,** 30° incidence, and 0° emission angle) using Hapke functions (Hapke 2012 and references therein). The global Hapke light scattering parameters have been iteratively derived from the Approach, Survey, and HAMO mission phases. Starting from the photometric model parameters presented by Reddy et al. (2015) iterations became necessary since increasing image resolution led to a significant increase of subpixel shadows, which change the weight of contributions from different latitudes to a global integrated model fit. Thus a transition from a one-parameter Henyey-Greenstein function to a two-parameter description (Shepard and Helfenstein, 2007) was required for HAMO data. In order to apply the geometric correction the HAMO stereophotogrammetry-based shape model using FC clear filter imagery (Preusker et al.,

2016) was used for image registration and local geometry computation. Tests with the LAMO shape model of Occator (Jaumann et al., 2017) revealed a number of small scale photometric errors that will require revision in the future. The resulting reflectance data are map-projected in several steps, and co-registered to align the color frames, to create color cubes used for our analysis. All FC color data used in this study have been obtained at LAMO orbit with an FC resolution of ~35 m/pixel.

A stereo-photogrammetry-based digital terrain model (DTM) with an area resolution of ~32 m/pixel and a height accuracy of ~1.5 m, covering Occator crater and its surroundings (3-36°N/223-256°E) (Jaumann et al. 2017) has been used for terrain analysis. The DTM was processed using the USGS Integrated Software for Imagers and Spectrometers (ISIS; Torson and Becker 1997). Before applying various boxcar filter functions (e.g., highpass, median, standard deviation), the DTM was projected equirectangular with the standard parallel at 19.5°N (i.e., the latitudinal center of the DTM) to achieve nearly true distances along latitudes. For equatorial equidistant cylindrical map projections true distances are only preserved along the meridians and the equator. Distortion along latitudes scales with the secant of latitude, e.g., at 75°N/S the measured (horizontal) distance has to be divided by 3.86. The maximum scaling factor for the DTM analysis is 1.04 at 16.5° from the standard parallel (i.e., at 3°N and 36°N). The rather small scaling factor makes this projection setting also suitable for slope analysis despite the equirectangular map projection not being a true conformal projection.

All data products were further analyzed using **Environmental Systems Research Institute (ESRI)** ArcGIS software. Reported dimensions of the central pit and dome are based on several

measurements using an azimuthal equidistant map projection centered at 19.66°N/239.61°E, where distances from the center point are represented correctly.

3. GEOLOGY OF OCCATOR

3.1. GEOLOGICAL SETTING

Occator (19.82°N, 239.33°E) is a ~92 km diameter[1] complex impact crater located on an elevated region named Hanami Planum, which extends from 14.5°S to 46.5°N with a longitudinal extent from 204°-263°E. It encompasses an area of approximately 500 km (N-S) by 460 km (E-W) and rises up to 6,145 m (31.7°N/212.9°E) above the best-fit ellipsoidal reference surface. The elevated area is resolved in gravity model data and is associated with the strongest negative Bouguer anomaly prevalent on Ceres (-250 mGal; Ermakov et al., in review). Ermakov et al. (in review) provide two hypotheses explaining the measured gravity anomaly: (1) a current buoyance-driven process below a thick shell or (2) a relatively low-density region below Hanami Planum.

3.2. INTERIOR

Occator is a complex crater, it exhibits a central pit (Ø ~9 km) surrounded by remnants of a central peak, and a flat floor bounded by a multitude of terraces (Nathues et al. 2015a, 2017a; Figs **2 - 9**). The central pit is up to 1 km deep and hosts the brightest surface feature on Ceres named Cerealia Facula (Fig. **5A**). The center of the pit is occupied by an asymmetric, fractured, and 3 - 3.5 km diameter dome, which rises up to 0.55 km above to lowest point (-1,220 m)

[1] IAU approved diameter and center coordinate.

within the pit. East of Cerealia Facula a number of less bright sites, collectively known as Vinalia Faculae mantle the

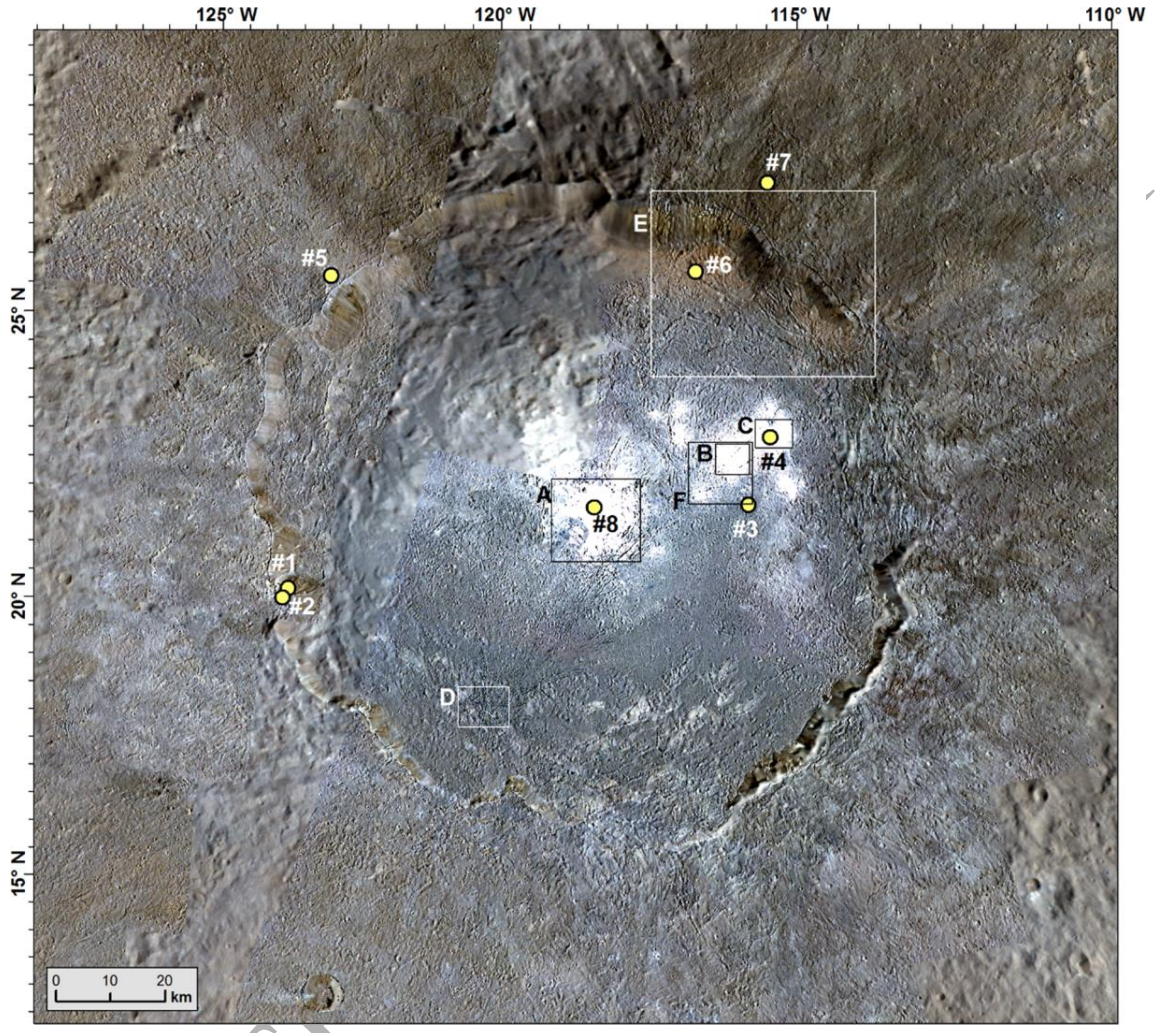

*Fig. **2**: Enhanced color mosaic of Occator crater. Data have been obtained at a resolution of ~35 m/pixel during LAMO orbit. Gaps in LAMO data are filled by HAMO imagery. RGB colors are R = 0.96 µm, G = 0.65 µm, and B = 0.44 µm* ***(red range: 0.020-0.035, green range: 0.021-0.038, blue range: 0.020-0.036). Dark floor and dark ejecta materials show higher relative reflectances at 0.44 µm and thus appear bluish. Ejecta located to the north-east are on average 1.5-times darker than typical dark material on Ceres (Thangjam et al. in review).*** *The crater exhibits terraced walls, a large flow deposit covering most of the crater floor, a central pit*

*containing a central bright dome (Cerealia Facula, **box A**), remnants of a central peak, and secondary bright spots **to its north-east** (Vinalia Faculae). Yellow dots mark those sites from which color spectra are shown in Fig. **14**. Boxes indicate displayed details of Figs **4 (F), 7 (E), 8 (D), 12 (A), 13A (B), 13B (C**). Equidistant cylindrical projection with the standard parallel at 19.5°N.*

distal portion of the largest lobate deposit within Occator (Figs **2** and **6B**; Nathues et al. 2017a). This lobate deposit — interpreted (here) to be a debris avalanche deposit — covers most of the floor and formed in consequence of a large collapse of the southeastern crater wall (Fig. **5**; Nathues et al. 2017a). Scully et al. (this issue) favor an impact melt origin of the lobate deposit. However, this interpretation is inconsistent with our age determinations in which the lobate deposit is significantly younger than the crater itself (Nathues et al. 2017a).

The surface texture of the large lobate deposit is smooth to knobby and at its distal NE portion hummocky (Fig. **3**). These textures are reflected in slope maps across several length scales. Figure **3**D shows the roughness (i.e., multi-slope) map of Occator's interior at length scales of 90 m (3 pixels; red channel), 510 m (17 pixels; green channel), and 2.91 km (97 pixels; blue channel). Note the slope values are calculated from median height values of 3×3, 17×17, and 97×97 pixel horizontal boxcars. The large lobate deposit appears black with subtle nuances of yellow and orange (Fig. **3**D). Black colors resemble here low slope values across all length scales whereas yellowish colors are characterized by low slope values on large length scales relative to high slope values on short to medium length scales. Similar surface roughness is also observed elsewhere within Occator. Portions of terrace material (i.e., material located between or

downslope of terrace blocks) as well as the small lobate deposit is located at the lower NE wall (Fig. **5**).

Interestingly, the NE wall and the proximal portion of the small lobate deposit appear slightly reddish in false-color RGB images (Fig. **7**). Here terrace material shows slightly different color spectra than elsewhere in Occator, which is a result of higher reflectivities longward of 0.65 µm. This spectral variation is likely not caused by compositional differences since the area is not distinct in VIR compositional maps (cf. Raponi et al., this issue). However, the presence of a mineral cannot be excluded that has not been detected yet on Ceres. Furthermore, surface roughness on photometrically effective scales (**much smaller than a meter**) seems to be higher for the regolith of the terrace material than on talus and floor materials, as indicated by subtle local differences in reflectance along seams of the HAMO mosaic.

Another way of highlighting surface textures by utilizing topographic data is the application of high-pass filters. In Figure **3**C, a 17×17 pixel boxcar high-pass filter is applied with 0.1% addback of the initial height value. The two lobate deposits as well as smooth terrace materials are easily depicted. Bright pixels highlight abrupt changes in slope, e.g., along the rim crest and terrace scarps and ridges.

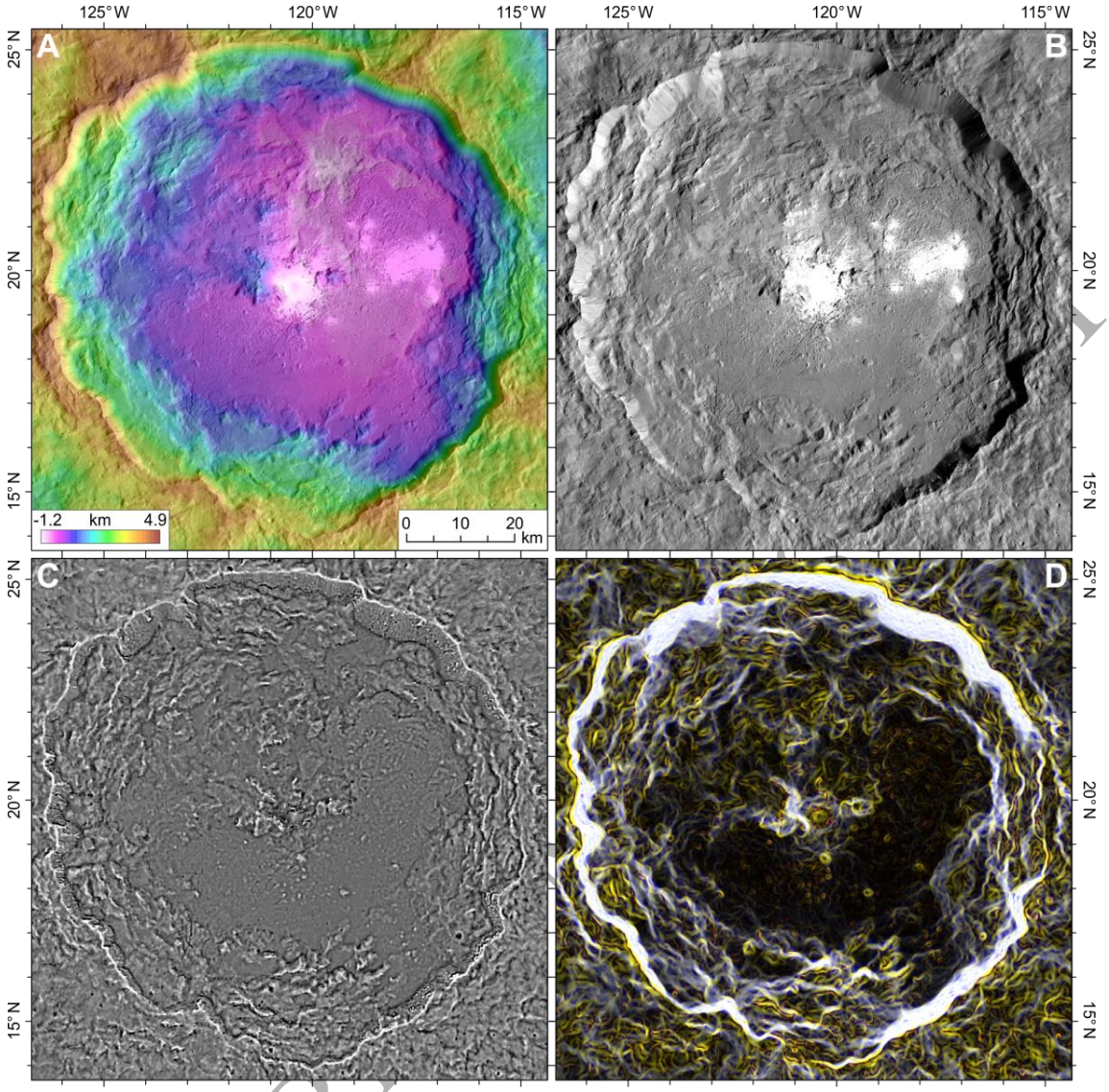

*Fig. **3**: Occator's interior.* ***(A) High-resolution LAMO DTM (32 m/pixel; Jaumann et al. 2017) of Occator superimposed on the LAMO FC clear filter mosaic (~35 m/pixel). (B) LAMO FC clear filter mosaic of Occator. (C) Highpass-filtered topography with 0.1% of the initial height value added back to the average value. (D) Map of decameter to kilometer-scale roughness. This RGB image represents slope values for median filtered topography using boxcar sizes of 3×3 pixels (90 m-length scale; Red), 17×17 pixels (510 m-length scale; Green), and 97×97***

pixels (2,910 m-length scale; Blue). Yellow hues indicate slope dominance on short to medium scales, bluish hues indicate higher slope values on medium to large scales relative to the short length scale, and black and white hues represent low and high slope values on all scales, respectively.

Bright material thickness of Vinalia Faculae has been first investigated by Nathues et al. (2017a). The material is rather thin, about a few meters or less, as it mostly mantles the rough surface texture of the large lobate deposit (Figs **5** and **6**B). The largest patches of bright material are associated with fractures at their periphery (Nathues et al. 2017a). Some fracture planes are coated with bright material and thus could be seen as sources. However, fractures near smaller bright patches are not observed at LAMO resolution. The fractures associated with Vinalia Faculae are characterized by circular to elliptical depressions of up to ~0.25 km in diameter. These depressions represent pits rather than impact features since they line up like a string of pearls along the fractures, which are ~0.11 – 0.18 km wide. Most fractures are about 50 - 100 m deep and only some portions of their bottoms get illuminated during a cerean day. By applying a non-linear image stretch, several small bright sites are resolved within the bright spots of Vinalia Faculae (Fig. **4**). These small bright sites at each bright spot (appearing dark in Fig. **4**) are interpreted to be cryovolcanic vents branching from a major conduit. It is currently unknown whether the conduits and fractures formed contemporaneously or consecutively.

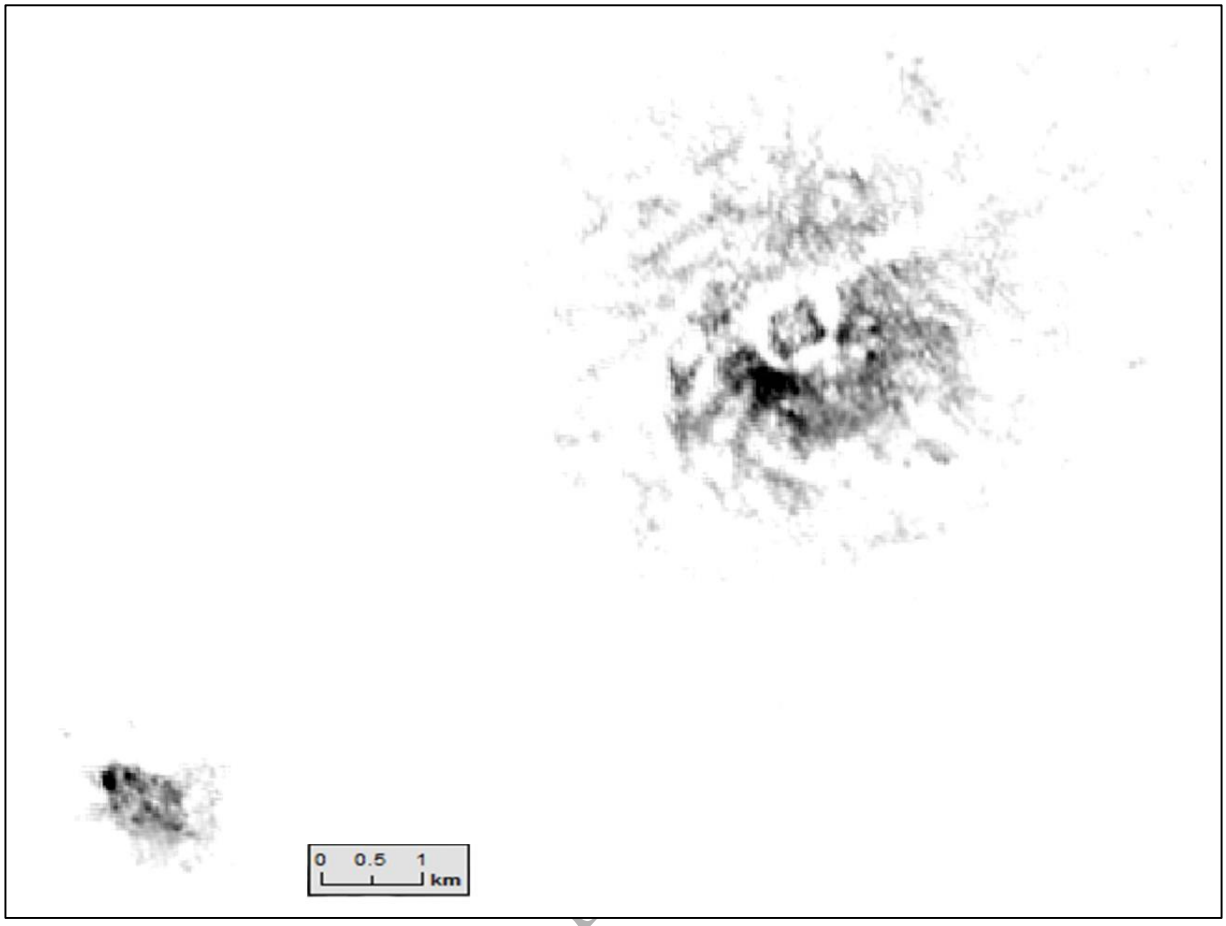

*Fig. **4**: Inverse stretch of two bright spots belonging two Vinalia Faculae (see box F in Fig. **2** for context). These faculae exhibit multiple small bright material concentrations which could be individual vents of larger conduits at depth.*

While the Vinalia faculae are rather thin deposits of bright material, the central pit consists of vast deposits. In particular, the dome is entirely composed of bright material (Figure **6**A and Nathues et al. 2017a). The formation ages of Cerealia Facula and the large (floor covering) lobate deposit are estimated on the basis of the exposed crater size–frequency distributions (Nathues et al. 2017a). While the crater wall collapse and subsequent formation of the large lobate deposit occurred at about 9 Ma, the bright material (including the dome) within the central pit formed at about 4 Ma (Nathues et al. 2017a, Neesemann et al. this issue). Regardless of the

crater counting results and used models, the morphology and appearance of bright material at the Occator faculae and the material on the floor and ejecta suggest that the bright material at Faculae is much younger compared to the rest of the impact crater material.

It is plausible to assume that the lobate deposit also covered previously existing bright material in the central pit (i.e., the pit was once deeper) since the debris avalanche was diverted to the NE and SW by central peak material (see Fig. **5**). Vinalia Faculae are entirely confined to the extent of the northeastern portion of the lobate deposit, and therefore, are younger than the deposit itself. The two largest bright sites of Vinalia Faculae (Figs **5** and **6**B) with area sizes of 14.7 km^2 and 13.5 km^2 were examined for superposed impact craters. Although none were detected at highest (LAMO) resolution, this information can still be used to derive a first-order model age. By applying Poisson timing analysis (Michael and Neukum 2010, Michael et al. 2016), median model ages of 690^{+1000}_{-500} ka and 760^{+1000}_{-600} ka are obtained, i.e., there is a 16% chance the deposits are older than ~1.7 Ma and a 16% chance them being younger than ~200 ka.

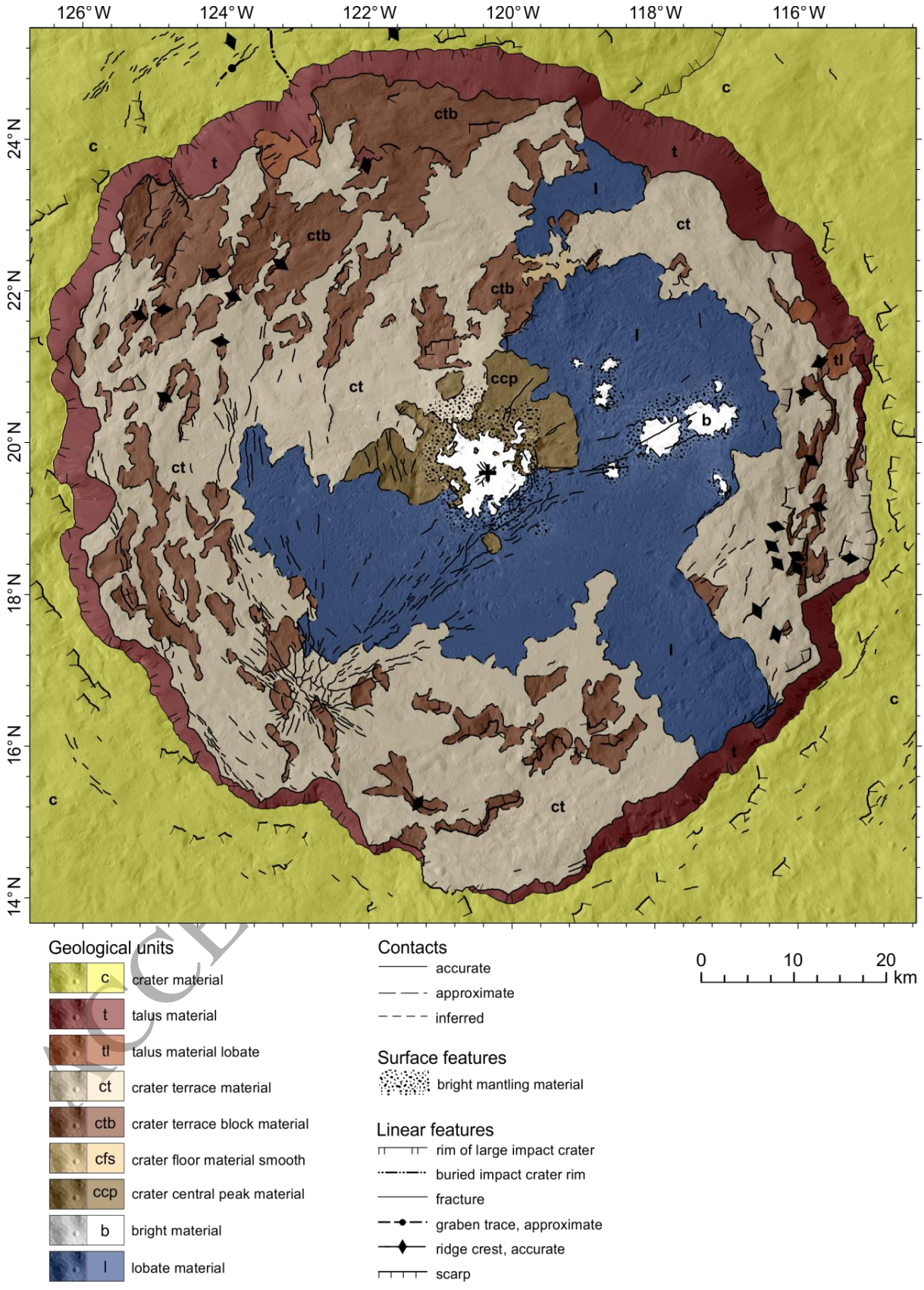
126° W
124° W
122° W
120° W
118° W
116° W
24° N
22° N
20° N
18° N
16° N
14° N
c
t
ctb
ct
l
ccp
b
tl
Geological units
c crater material
t talus material
tl talus material lobate
ct crater terrace material
ctb crater terrace block material
cfs crater floor material smooth
ccp crater central peak material
b bright material
l lobate material
Contacts
accurate
approximate
inferred
Surface features
bright mantling material
Linear features
rim of large impact crater
buried impact crater rim
fracture
graben trace, approximate
ridge crest, accurate
scarp
0
10
20
km

*Fig. **5:** Simplified geological map of the interior of Occator crater (modified after Nathues et al. 2017a). The interior is dominated by terrace blocks (ctb) and unconsolidated terrace material (ct). Lower terrace materials in the center of the crater are buried by a large lobate deposit (l), which formed in consequence of a large SE wall collapse. Note that some margins of the lobate deposit are buried by subsequent unconsolidated terrace materials. Wall failure to the NE also formed a smaller debris avalanche deposit (i.e., lobate deposit). For further details the reader is referred to Nathues et al. (2017a).*

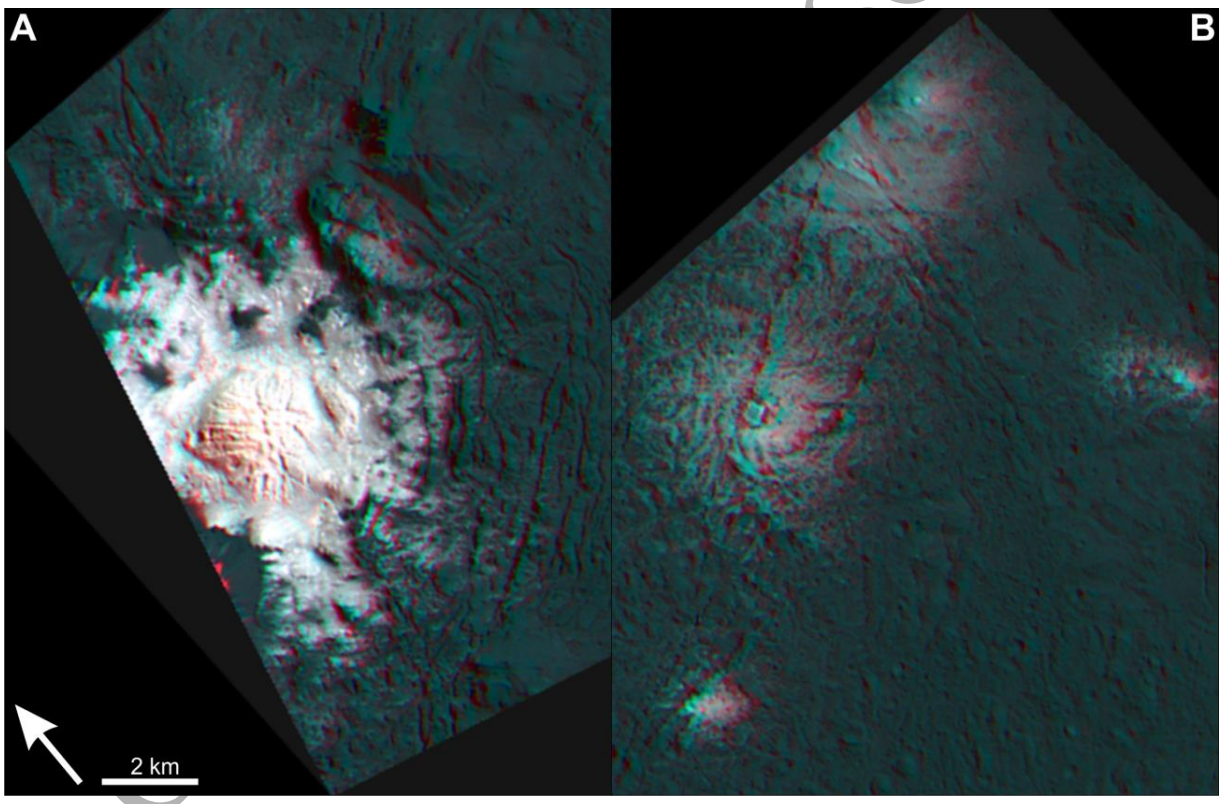

*Fig. **6:** False-color anaglyphs of Cerealia Facula (A) and Vinalia Faculae (B) (R = 0.96 µm, G = 0.65 µm, B = 0.44 µm; ~35 m/pixel resolution). Bright material in Vinalia Faculae is associated with fractures. Some fracture planes are covered with bright material. Arrow points to north in both scenes. Scale bar applies to A and B.*

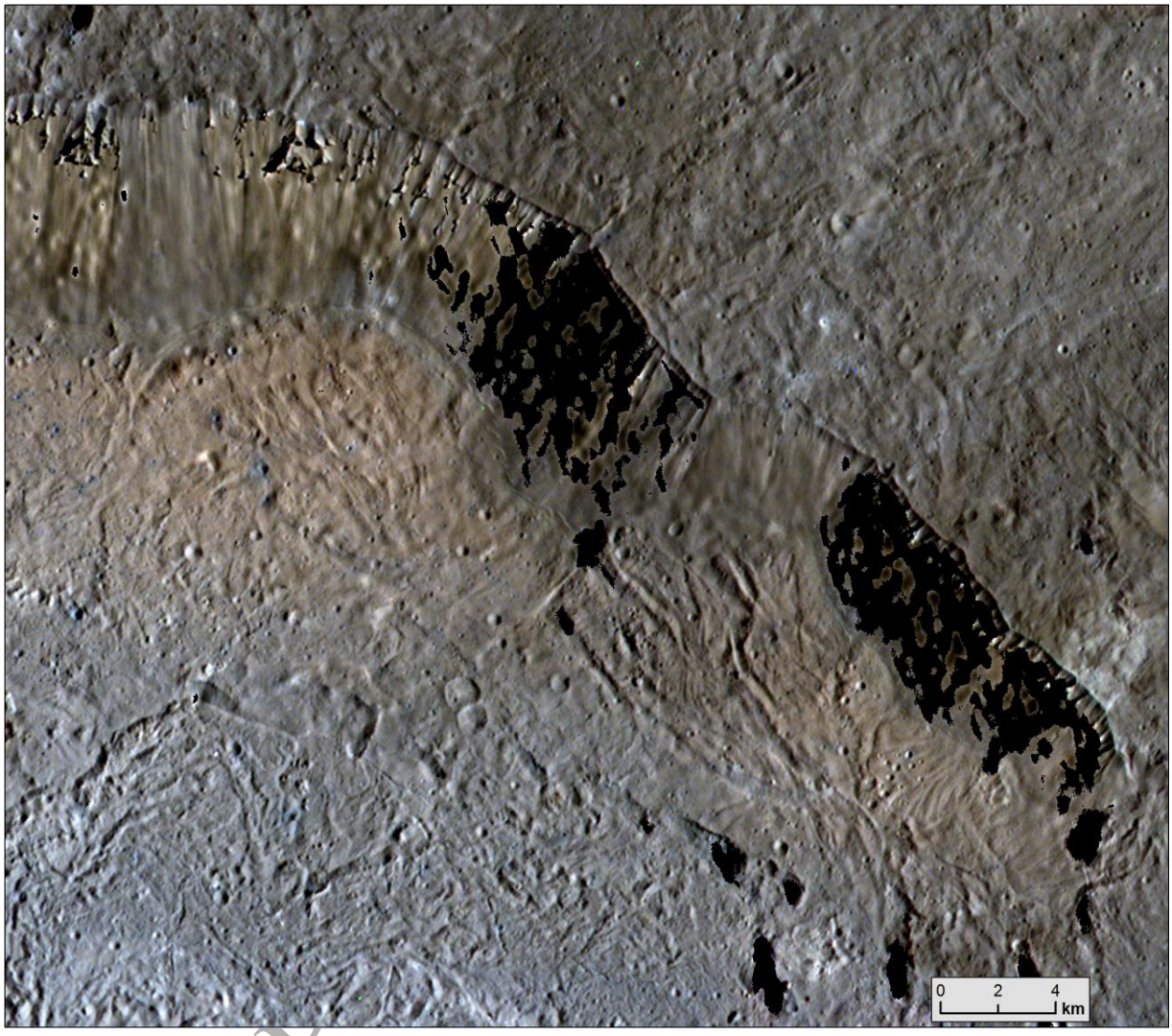

*Fig. **7:** Color mosaic of the northeastern wall of Occator. RGB colors are R = 0.96 µm, G = 0.65 µm, and B = 0.44 µm (~35 m/pixel resolution, LAMO orbit, **same stretch as in Fig. 2**, see box E in Fig. **2** for context). Wall height is up to 3.9 km. Large-scale downslope mass-movements and formation of lobate deposits are observed at the base of the wall (cp. Fig. **5**). The crater wall, terrace, and lobate materials in this area exhibit a distinct color compared to the crater floor and other terrace materials within Occator. Black areas represent no data as a result of a limited photometric correction due to high local slopes.*

Two large fracture systems intersect within southwestern terrace material (Fig. **8**, Buczkowski et al. this issue, Nathues et al. 2017a). The one system extends towards the northeast across the large lobate deposit while the other system indicates a concentric pattern with individual fracture segments being oriented parallel to crater wall segments. A similar concentric fracture pattern is also observed on the crater rim (Buczkowski et al. 2016, Nathues et al. 2017a) and are likely precursor fractures for future partial crater wall collapses (Nathues et al. 2017a). At the terminus of the NE-trending fracture system the two largest bright areas of Vinalia Faculae are present (Fig. **6**B). It is noted that individual fractures are also associated with the central pit. The concentric fractures at the southeastern pit rim are potentially associated with the emplacement of the large lobate deposit while those prevalent on remnant central peak material are clearly associated with the formation of the pit (and destruction of the peak) (Nathues et al. 2017a).

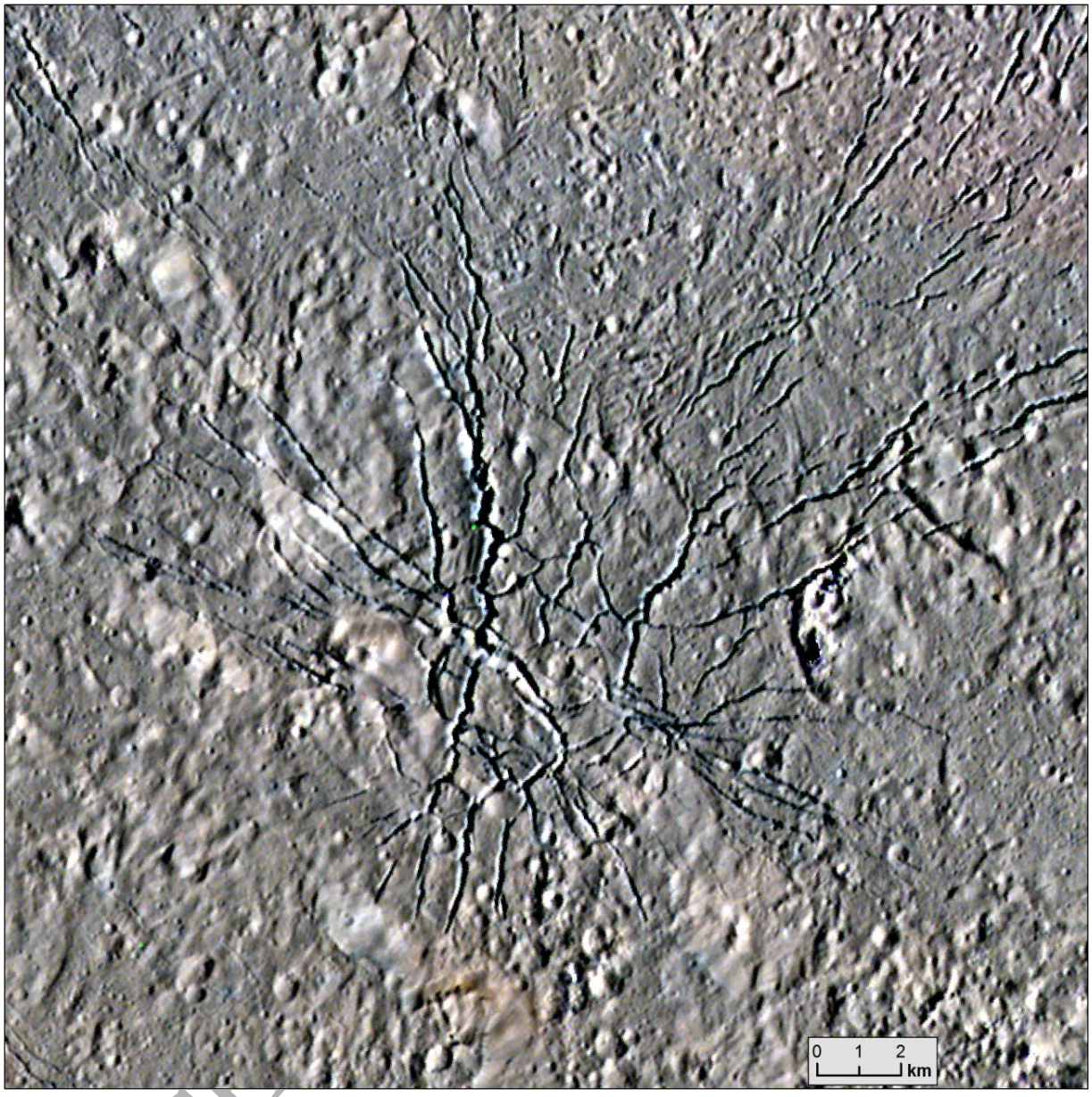

Fig. ***8****: Color mosaic of fractures at the SW portion of the crater floor. RGB colors are R = 0.96 µm, G = 0.65 µm, and B = 0.44 µm (~35 m/pixel resolution; LAMO orbit,* ***same stretch as in Fig. 2****). Two fracture systems intersect at the southwestern crater floor (see box D in Fig.* ***2*** *for context). The fractures are likely caused by updoming (Buczkowski et al., 2016; Nathues et al. 2017). Color variation across the scene is subtle. North is up.*

3.3. EJECTA MATERIAL

The ejected material of Occator crater exhibits a distinct color and reflectance dichotomy (ranging between ~0.02 and ~0.05 at 0.55 µm), which is approximately oriented NE-SW (Figs 2 and **9**). The eastern portion appears darker in RGB colors whereas the western half is characterized by predominantly bluish appearing material (Fig. **9**E), which is typical for fresh to moderately degraded craters on Ceres (cf. Nathues et al. 2016; Schmedemann et al. 2016). Regardless of color and reflectance variations across the continuous ejecta blanket, the surface texture is generally smooth. Fluidized ejecta as observed at other fresh craters on Ceres (Krohn et al., 2016; Platz et al., in press) are not observed. The frequently found hummocky texture in medial to distal reaches is primarily caused by the pre-existing cratered terrain, i.e., the ejecta blanket mantles the terrain, and therefore, traces pre-existing terrain roughness. Fractures within ejecta material are located circumferential to the crater rim and likely resemble precursor wall-failure structures (Nathues et al., 2017a). To the west, fractures are also observed above large buried craters and likely developed as the result of material sagging and/or compaction.

The proximal to medial ejecta blanket is sufficiently thick to be detectable in the LAMO topography data and extends up to one crater diameter (i.e., ~92 km) from the crater rim (Fig. **9**B-D). Due to the ejecta's smooth texture and sufficient thickness to bury smaller pre-existing craters, the annulus is clearly visible (Fig. **9**D). The distal continuous ejecta, however, shows an asymmetric distribution and extends much farther from the crater rim (Fig. **10**). To the east and north it extends to approximately 140 km (roughly three crater radii) whereas to the south and west ejecta is visible to distances up to 190 km (about four crater radii). Individual crater rays can be traced in LAMO clear filter imagery to distances of more than 500 km, i.e., approximately 11 crater radii (Fig. **11**). The texture of these rays is similar to other rayed craters such as Haulani

(Platz et al., in press). The pronounced ejecta asymmetry is the result of the high rotation rate of Ceres (9.07h; for ejecta simulations see Platz et al. (2016) and Schmedemann et al. (2017)).

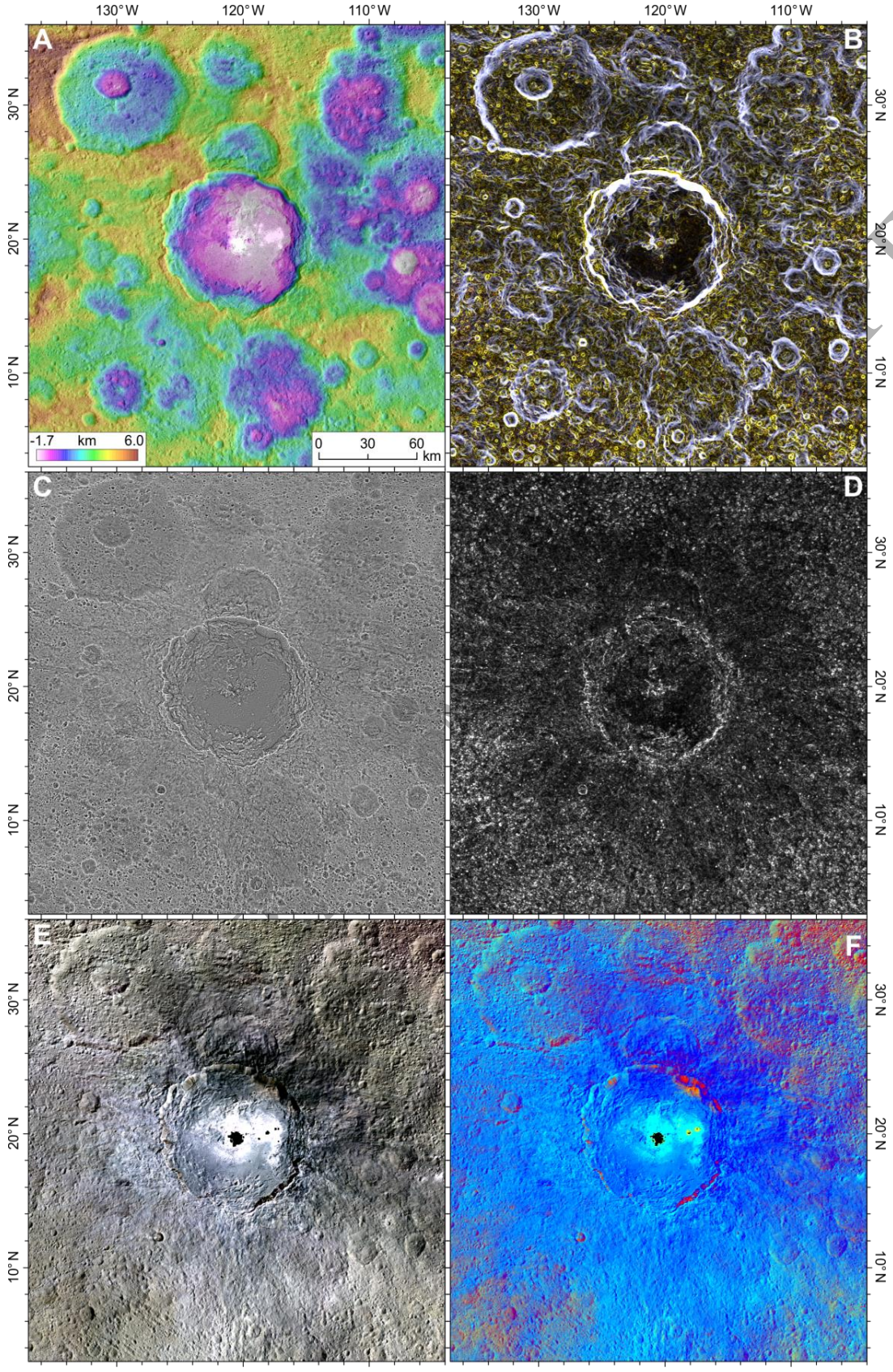
130° W
120° W
110° W
30° N
20° N
10° N
A
B
C
D
E
F
-1.7 km 6.0
0 30 60 km

Fig. ***9****: Illustration of the proximal to medial ejecta extent of Occator crater using different data products. (A) High-resolution LAMO DTM (32 m/pixel; Jaumann et al. 2017) of Occator and surroundings superimposed on the LAMO FC clear filter mosaic (~35 m/pixel). (B) Map of decameter to kilometer-scale roughness. This RGB image represents slope values for median filtered topography using boxcar sizes of 3×3 pixels (90 m-length scale; Red), 17×17 pixels (510 m-length scale; Green), and 97×97 pixels (2,910 m-length scale; Blue). Yellow hues indicate slope dominance on short to medium scales, bluish hues indicate higher slope values on medium to large scales relative to the short length scale, and black and white hues represent low and high slope values on all scales, respectively. (C) Highpass-filtered topography with 0.1% of the initial height value added back to the average value. Note that pre-existing small-scale diameter craters are largely invisible within proximal to medial ejecta material. (D) Standard deviation of heights from a 17×17 pixel median filtered and detrended topography. The black annulus extending approximately 1-2 crater radii from the rim crest represents the thick and continuous proximal to medial ejecta blanket. (E) Enhanced HAMO RGB image (R=0.96 µm, G=0.75 µm, B=0.44 µm) with black and bluish appearing ejecta material whose extent is largely confined to the proximal to medial ejecta extent shown in (D). (F) False-color ratio map (R=0.96/0.44 µm, G=0.65 µm, B=0.44/0.96 µm;* ***same stretch as in Fig. 10****) with Occator ejecta material highlighted in blue. Note that blueish colors extend beyond the annulus shown in (D). This indicates that distal (thin) ejecta were deposited more than one Occator diameter from the rim. Individual ejecta rays can be traced to distances of up to 500 km from Occator's rim (cp. Figs* ***10*** *and* ***11****). All panels show the exact same extent of Ceres' surface centered at Occator crater from 3-36°N and 223-256°E. Black dots in panels E and F represent saturated pixels. Equidistant cylindrical projection with standard parallel at 19.5°N.*

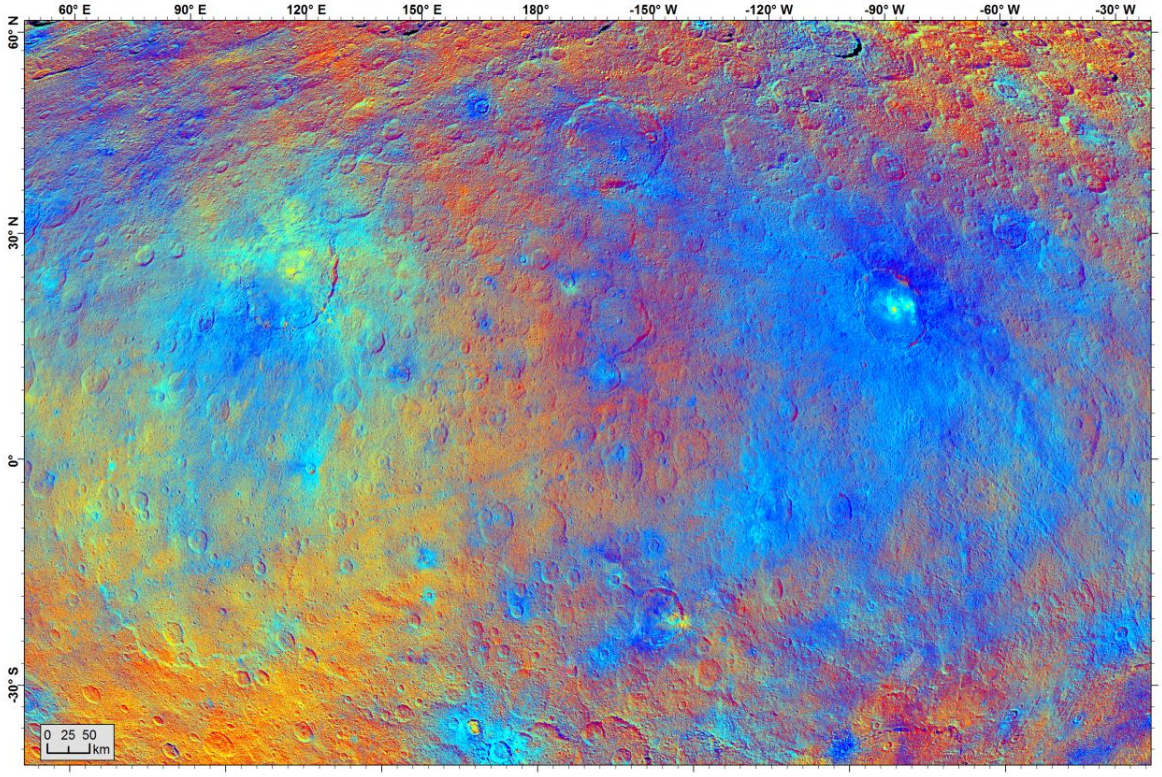

Fig. ***10****: False color-ratio map (R= 0.96/0.44 µm, G= 0.65 µm, B= 0.44/0.96 µm* ***(red range: 0.98-1.09, green range: 0.027-0.037, blue range: 0.91-1.02)*** *of Occator ejecta. Mosaic resolution is ~140 m/pixel (HAMO orbit). Mollweide projection centered at 0°N/180°E. The bluish ejecta field of Occator is easily visible. Crater rays extend several hundred kilometers to the southwest. For a close up view of the nearby ejecta see Figs 2, and* ***9****F.*

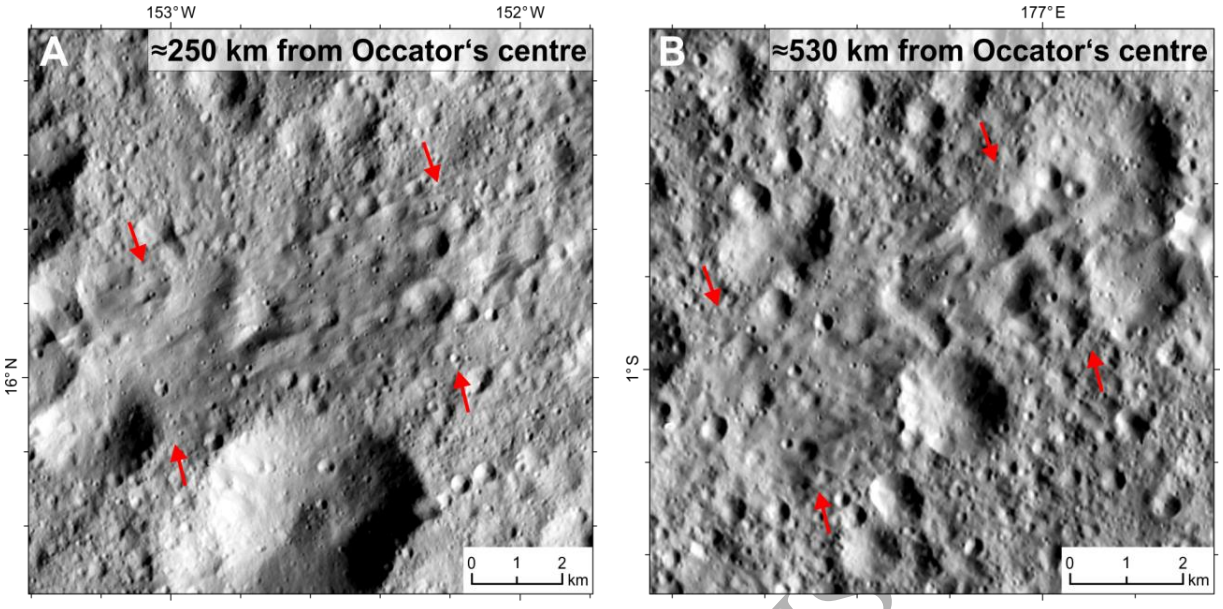

*Fig. **11:** Distant ejecta rays of Occator as seen in FC clear filter images (~35 m/pixel). Arrows in panels (A) and (B) confine the northern and southern extent of far-flung ejecta materials. The smooth texture and thin thickness of crater rays is noted.*

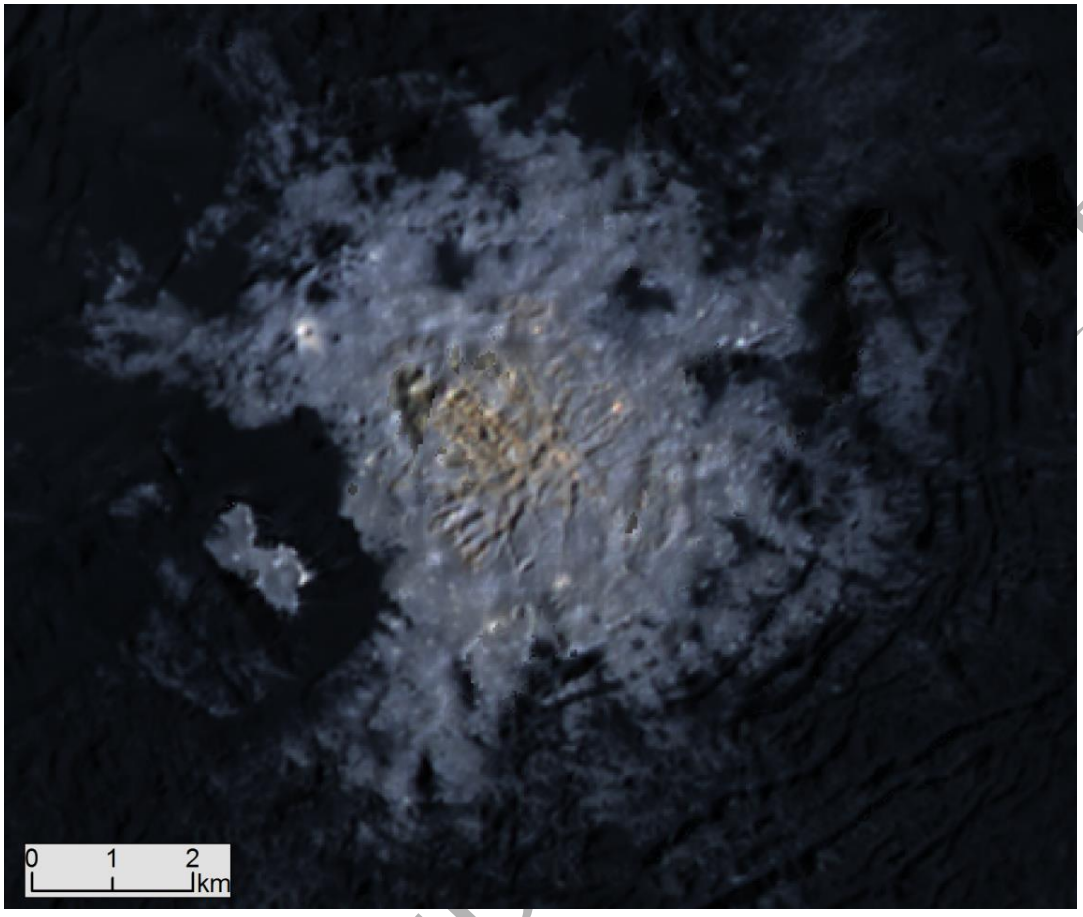

Fig. ***12****: Color mosaic of Cerealia a Facula from LAMO orbit (resolution ~35 m/pixel). RGB colors are R = 0.96 µm, G = 0.65 µm, and B = 0.44 µm* ***(red range: 0.009-0.598, green range: 0.0-0.579, blue range: 0.01-0.45)****. Photometric correction has been performed by using the LAMO DTM (Jaumann et al. 2017). A significant fraction of the pit is covered with bright material which has been deposited likely by one or more eruptive events. Isolated bright material is located at several elevated areas. The central dome shows radial fractures. Further fractures are associated with the central collapse (pit). North is up. Fig.* ***2*** *shows the context of this scene (box (A)). Equidistant cylindrical projection with the standard parallel at 19.5°N.*

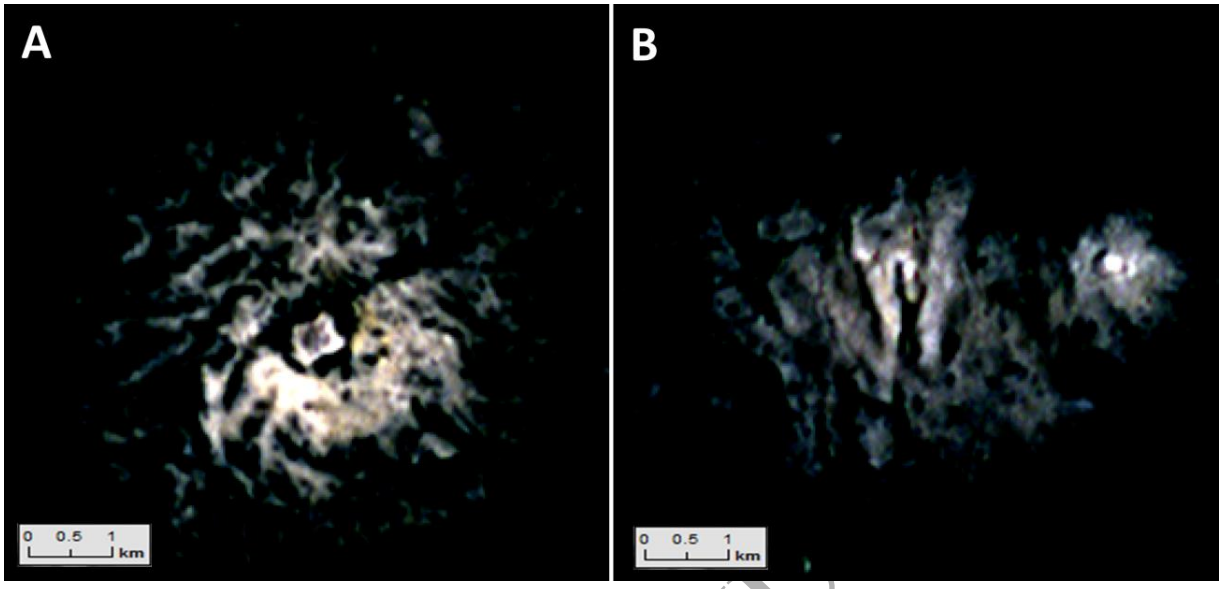

*Fig. **13**: Enhanced color mosaics of the largest two bright spots of Vinalia Faculae. Data have been obtained from ~370 km distance during LAMO orbit (~35 m/pixel resolution). RGB colors are R = 0.96 µm, G = 0.65 µm, and B = 0.44 µm **(red range: 0.097-0.158, green range: 0.097-0.171, blue range: 0.09-0.145)**. (A) Western spot, containing a nearly rectangular bright central feature and a bright area surrounding the center (see box B in Fig. **2** for context). (B) Eastern spot, containing a V-shaped fracture (running south to north) from which the bright material seems to originate (see box C in Fig. **2** for context). Color variation within and among Vinalia Faculae spots is marginal. North is up.*

4. COLOR VARIATION

The floor of Occator shows the highest reflectance contrast on Ceres ranging between ~0.02 and >0.3 @0.55 µm. While the faculae and dark floor areas have been described in detail in Nathues et al. (2017a)**,** we now focus on some further surface features associated with Occator. For the

present analysis we investigated FC color cubes covering the wavelength range 0.4 – 1.0 µm and resolve spectral details down to ~35 m/pixel.

It was shown by Nathues et al. (2017a) that color spectra of the central bright dome are red sloped throughout the FC wavelength range, while bright material outside the dome is slightly blue sloped longward of 0.65 µm (e.g., #4, Fig. **14**). Further color spectra of Occator are plotted in Fig. **14**. Bright material color spectra of the inner wall (e.g., #1) and ejecta (e.g., #5) of Occator exhibit typically lower reflectances than bright material floor spectra (e.g., #4). Bright material spectra of all sites at Occator, except for the dome, are blue sloped longward of 0.55 µm and show here slope variations. Faculae bright material is dominated by the sodium carbonate component (De Sanctis et al. 2016, Nathues et al. 2017a, Palomba et al. this issue).

All dark material sites at Occator show similar spectral shapes in FC wavelengths. The spectra are in general slightly red sloped between 0.44 and 0.65 µm and slightly blue sloped at longer wavelengths (e.g., #2, #3, #6, #7 in Fig **14**). However, the northwestern wall material (#6, Fig **14**) is within the spectral uncertainties neutrally sloped longward of 0.55 µm and thus slightly different in color (see Fig. **7**).

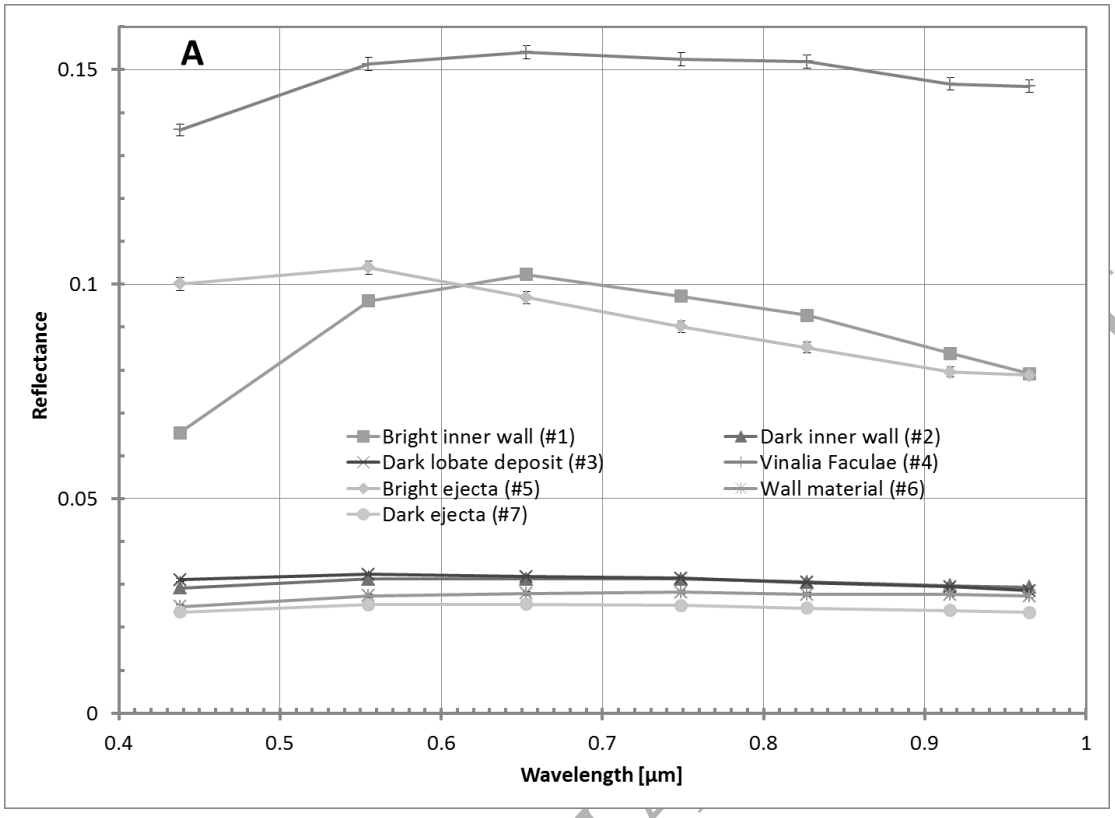
A
Reflectance
Wavelength [µm]
0.15
0.1
0.05
0
0.4
0.5
0.6
0.7
0.8
0.9
1
Bright inner wall (#1)
Dark inner wall (#2)
Dark lobate deposit (#3)
Vinalia Faculae (#4)
Bright ejecta (#5)
Wall material (#6)
Dark ejecta (#7)

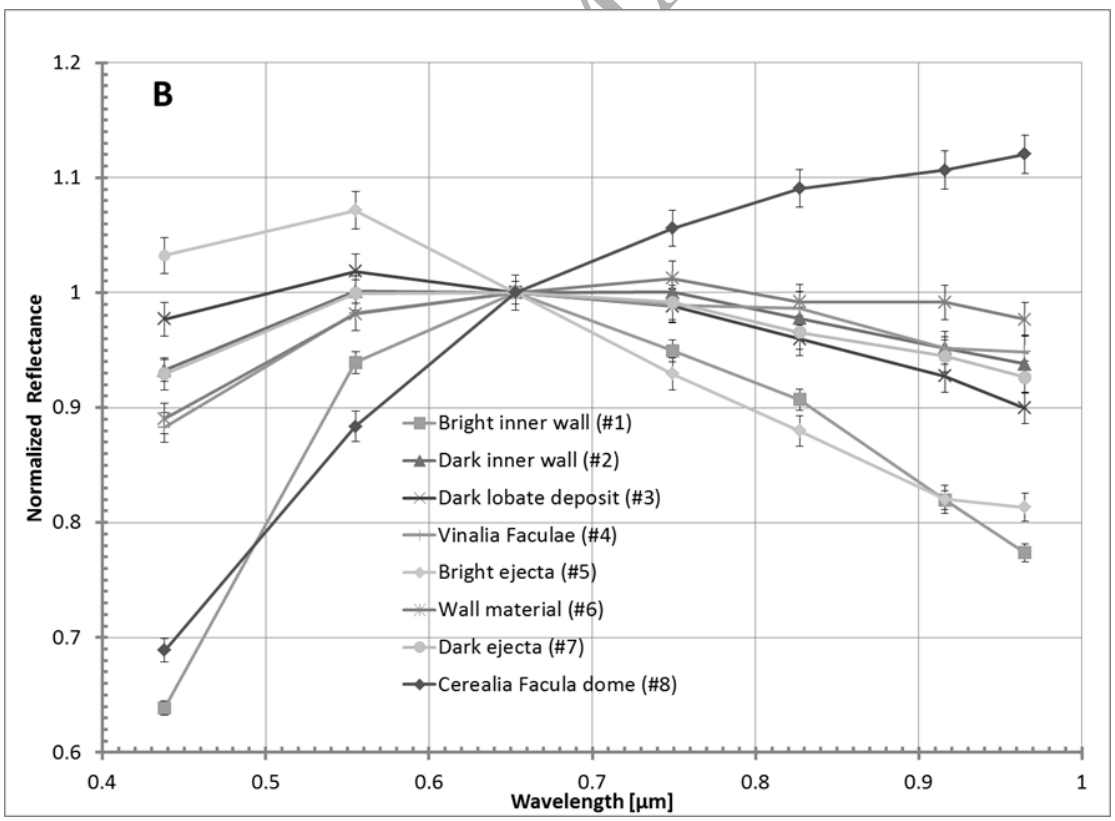
B
Normalized Reflectance
Wavelength [µm]
1.2
1.1
1
0.9
0.8
0.7
0.6
0.4
0.5
0.6
0.7
0.8
0.9
1
Bright inner wall (#1)
Dark inner wall (#2)
Dark lobate deposit (#3)
Vinalia Faculae (#4)
Bright ejecta (#5)
Wall material (#6)
Dark ejecta (#7)
Cerealia Facula dome (#8)

Fig. ***14****: FC color spectra of different color units in Occator. Each spectrum represents an average of a specific region of interest (ROI). Locations of ROIs are marked in Figure 2. (A) Reflectance values versus wavelength. Spectrum #8 (Nathues et al. 2017a) is outside the displayed range (reflectance of 0.38 at 0.55µm) and thus not shown in panel A. Statistical errors are on the order of symbol size. (B) Reflectances normalized at 0.65 µm. Color spectra of dark material across the crater are very similar showing only minor spectral slope variation and are similar to the global average spectrum (Thangjam et al., in review). Bright material spectra outside the dome are mainly mixtures of two endmember spectra: entirely red sloped spectra of the bright dome material and dark background material spectra (Nathues et al. 2017a).*

5. DISCUSSION

The distribution of the faculae in the central and eastern part of Occator's floor indicates non-uniformity: either the ascending brine is irregularly distributed below the floor, or the floor material thickness significantly varies. In favor of the latter view is the presence of the radial fracture systems on the south-western floor (Fig. **8**), which is probably caused by domical uplift (Buczkowski et al. 2016). Apparently a similar kind of activity caused by a subsurface reservoir like at Vinalia Faculae (Nathues et al. 2017a, Ruesch et al., this issue) is acting in the south-west, but has either stopped or is in an earlier stage than at Cerealia Facula, since bright material did not reach in significant amounts the surface (yet) – only some small slightly brighter areas cover a few of the fracture planes. Possibly a thicker overlying surface layer prevented extrusion despite local uplift. Thus the presence of one or more substantial brine reservoirs in conjunction with ancient regional fractures and conduits were the pre-requisite for the outstanding, long-

lasting unique activity after the impact (Nathues et al. 2017, Quick et al. this issue, Bowling et al. this issue). Alternatively, the uplift in the south-western portion of Occator could be due to brine freezing (i.e., volume expansion) at depth rather than upwelling material.

Often shadows do not allow deeper views into the fractures, but the high concentration of bright material, appearing reddish in 'clementine colors' (Fig.**15**), next to some fractures to the north-east, indicate that these or associated conduits are probably the source vents; especially since some of the fracture planes are coated with bright material. On the contrary, there is no obvious correlation of bright material and tiny impact craters near Vinalia Faculae (see arrows in Fig. **15**). This can be interpreted in terms of the thickness of the bright material and the mechanism of deposition. At the craters near Vinalia Faculae a bright sub-surface layer is not exposed by those small impacts, likely a bright surface layer is not present at all, despite a considerable presence of bright material on the surface. Thus the brine extruded from localized fractures/vents, which are only resolved by FC images in cases of the largest deposits. Smaller deposits of reddish (Fig. **15**) carbonate-rich material, which show up near the major Vinalia Faculae spots, often cannot be linked to resolved fractures or vents.

Our observations are in accordance with a brine fountain origin of salts deposits. Brine moving towards the surface through a vent or a fracture will produce droplets once the pressure release in the ascending brine allows boiling. Due to the large surface of the mechanically disrupted liquid the solvent (H_2O) disappears immediately leaving behind crystallized solutes, i.e. salt minerals. In this scenario, the grain size of the salt is expected to be particularly small since the instantaneous loss of water does not allow crystal growth.

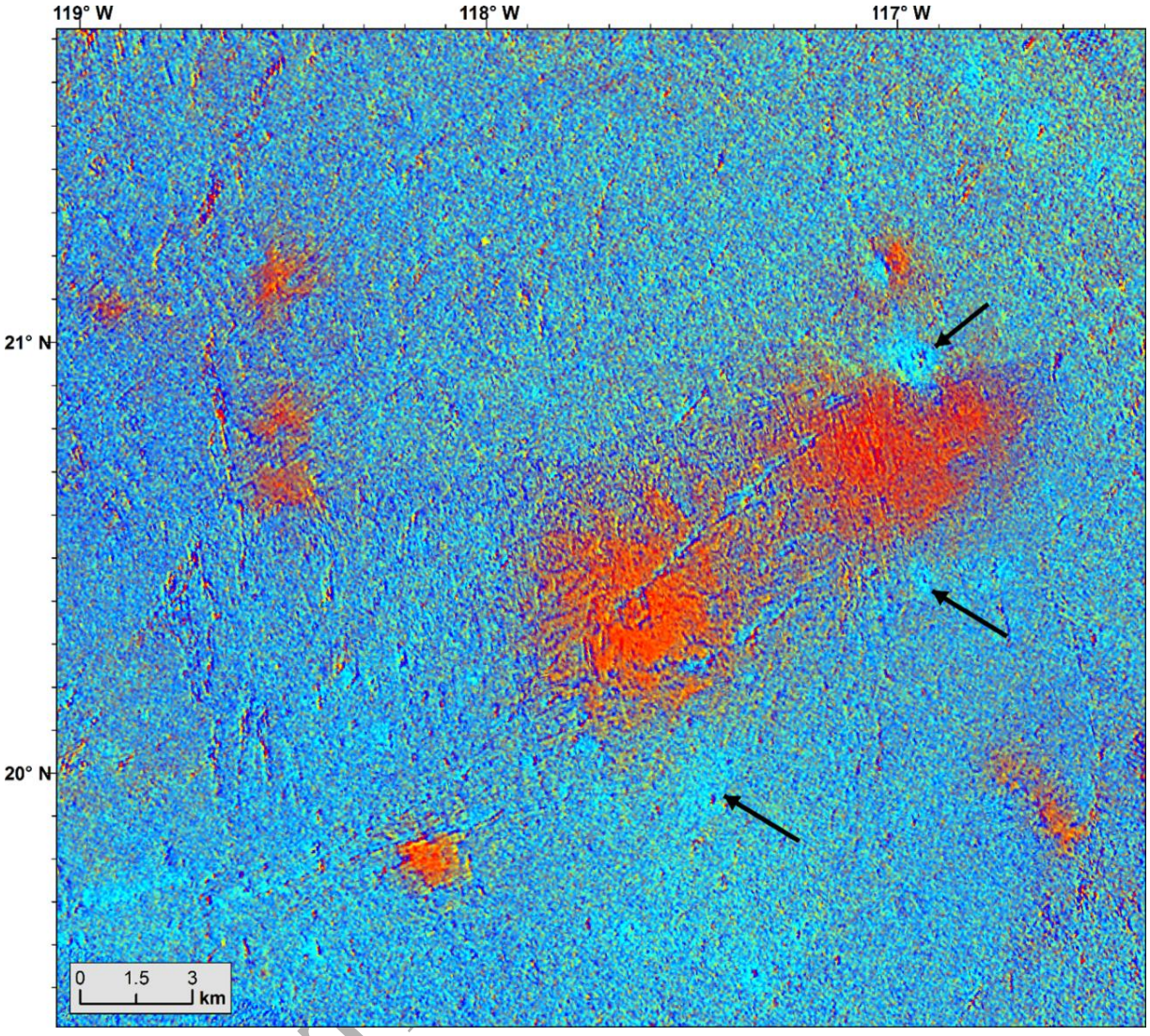

Fig. ***15****: Vinalia Faculae in "Clementine colors" (R=0.65µm/0.44 µm, G=0.65 µm/0.92 µm, B=0.44 µm/0.65 µm* ***(red range: 0.938-1.118, green range: 0.996-1.137, blue range: 0.889-1.064)****. Note the bluish little craters (arrows) which did not excavate carbonate-rich material (here red-appearing).*

In summary, the interior of Occator crater exhibits evidence of present and past endogenic activity, millions of years after crater formation (Nathues et al. 2017a). This view is supported by our present study which defines, for the first time, the maximum age of the Vinalia Faculae:

these spots are likely less than 2 Ma old and thus represent the youngest (known) carbonate deposits on Ceres. The overall characteristics of Cerealia and Vinalia faculae are consistent with a cryovolcanic origin (Nathues et al. 2017a, Ruesch et al. this issue**)**. The central pit of Occator, its dome, and the smaller bright spots (i.e., Vinalia Faculae) covering the distal portion of the debris avalanche deposit are composed of bright carbonates (De Sanctis et al. 2016) — material that is essentially uncontaminated by ambient dark material. It seems likely that multiple extrusive events caused deposition of these bright carbonates. While the central pit activity was clearly of an eruptive nature, the type of activity that formed Vinalia Faculae is less certain. Either these bright spots also formed due to eruptive processes (Ruesch et al. this issue) or by outgassing and/or sublimation processes (Nathues et al. 2017a). The forces leading to this activity might not be directly linked to the heat introduced by the impact, since cooling **occurred on shorter time scales** (see Bowling et al. this issue) but indirectly due to mass-removal and long lasting processes of gas exsolution.

According to evolution models (e.g. Castillo-Rogez 2011, Travis et al. 2015) and recent Dawn findings (Prettyman et al. 2016) Ceres today contains large amounts of H_2O in the form of an icy mantle and possibly a large liquid reservoir (‘ocean’) at depth. Thus modeling (Bowling et al. this issue, Quick et al. this issue) and observations support the existence of brine reservoirs at depth from which carbonates, now found on the surface, could originate. Brine has been transported through conduits and vents to the surface.

The presence of carbonate-bearing bright spots on the floors of several other deep, young craters (Stein et al., this issue, Palomba et al., this issue) supports the notion that extant subsurface brine reservoirs may be widespread across Ceres. The lack of carbonate-bearing bright spots in some large and deep craters (e.g. Vinotonus, Urvara) indicates that such subsurface brines may be

deposited non-uniformly and/or be unable to reach the surface in some craters. Although other bright spots on crater floors likely formed via impact-induced heating and upwelling of subsurface volatiles (Stein et al., this issue), none show clear signs of eruptive processes as seen in Cerealia Facula. This may indicate that most of the bright spots on crater floors form by excavation and that eruptive activity is unique to **Occator's** Cerealia Facula. In this context it is important to mention that Cerealia Facula is made of 45 - 80 volume % sodium carbonate (De Sanctis et al. 2016, Palomba et al. this issue)**,** which is unique on Ceres. Alternatively, the lack of ancient (pre-impact) fractures in other craters that provide a conduit for brines to reach the surface could be the reason for the lack of Occator-like faculae. Further it seems possible that signs of eruptive activity around other bright spots may have been removed via lateral material mixing, space weathering, and/or other processes.

6. Conclusions

Occator is a complex central pit impact crater hosting intriguingly bright faculae of cryovolcanic origin (e.g., Nathues et al. 2017a, Scully et al. this issue). These faculae are sodium carbonate-rich deposits, briny liquids emplaced on the surface from reservoir(s) at depth (Nathues et al. 2017a). Intrusions of brine formed fractures, conduits and vents through which the material reached the surface. The central facula is located in a central pit exhibiting a central dome that shows indications of geologically recent eruptive processes. Most other faculae of Occator are located on a young, large lobate deposit that possibly originated from a major wall collapse. The upper age limit of these faculae is ~2 Ma. Color spectra of the faculae range from entirely red-sloped dome spectra to blue sloped spectra longward of 0.65 µm for the remaining bright areas. Floor and dark

material color spectra are similar with nuances in blue and red spectral range. The ejecta of Occator exhibits a color and reflectance dichotomy, i.e. the north-eastern ejecta is darker, while the western is brighter and appears bluish in our RGB color mosaics. Ejecta material extends up to 140 km, in some cases to up to 500 km from the crater center. Two major fracture systems within the southwestern terrace material show signs of updoming, possibly due to similar processes as in Occator's center. The NE wall and proximal small lobate deposits are different in color compared to the majority of wall and floor materials. This difference is due to physical parameter differences of the regolith rather than mineralogical variations.

7. ACKNOWLEDGEMENTS

We thank the Dawn operations team for the development, cruise, orbital insertion, and operations of the Dawn spacecraft at Ceres. Also we would like to thank the Framing Camera operations team, especially P. G. Gutierrez-Marques, J. Ripken, I. Hall, and I. Büttner. **Frank Preusker is particularly acknowledged for producing the Occator Digital Terrain Model at LAMO resolution.** The Framing Camera project is financially supported by the Max Planck Society and the German Space Agency, DLR.

8. References

Bowling et al. this issue

Buczkowski, D.L. et al. 2016 The Geomorphology of Ceres. Science 353. Issue 6303, aaf4332.

Buczkowski, D. L. et al., this issue.

Castillo-Rogez, J. C. 2011, Ceres – Neither a Porous nor Salty Ball. Icarus 215, 599-602.

Combe, J.-P. et al. 2016. Detection of Local H_2O Exposed at the Surface of Ceres. Science 353, Issue 6303,aaf3010..

Combe, J.-P., et al. Exposed H_2O-rich Areas Detected on Ceres with the Dawn Visible and Infrared Mapping Spectrometer. Icarus (submitted).

De Sanctis, et al. 2016. Bright Carbonate Deposits as Evidence of Aqueous Alteration on (1) Ceres. *Natur* 536, 54-7.

Ermakov, A.I. et al. Constraints on Ceres' Internal Structure and Evolution from its Shape and Gravity Measured by the Dawn Spacecraft. JGR (submitted).

Hapke, B., 2012. Theory of Reflectance and Emittance Spectroscopy. Cambridge UK, Cambridge University Press

Jaumann, R. et al. 2017. Topography and Geomprphology of the Interior of Occator Crater on Ceres. Lunar Planet. Sci.XLVIII, id.1440.

Krohn, K., 2016. Cryogenic Flow Features on Ceres: Implications for crater-related Cryovolcanism. Geophys. Res. Lett., 43, 11994-12003.

Michael, G. G., Neukum, G. 2010. Planetary Surface Dating from Crater Size-Frequency Distribution Measurements: Partial Resurfacing Events and Statistical Age Uncertainty. Earth Planet. Sci. Lett. 294, 223-229.

Michael, G. G., Kneissl, T., Neesemann, A.2016. Planetary Surface Dating from Crater Size-Frequency Distributions: Poisson Timing Analysis. Icarus 277, 279-285 .

Nathues, A., et al. 2014. Detection of Serpentine in Exogenic Carbonaceous Chondrite material on Vesta from Dawn FC Data. Icarus 239, 222-237.

Nathues, A., et al. 2015a. Sublimation in Bright Spots on (1) Ceres.*Natur* 528, 237-240.

Nathues, A. et al. 2015b. Exogenic Olivine on Vesta from Dawn Framing Camera Color Data. Icar 258, 467 – 482.

Nathues, A. et al. 2016. FC Colour Images of Dwarf Planet Ceres Reveal a Complicated Geological History. *P&SS* 134, 122-127.

Nathues, A., et al. 2017a. Evolution of Occator Crater on (1) Ceres. The Astronomical Journal, 153.

Nathues, A., et al. 2017b. Oxo Crater on (1) Ceres—Geologic History and the Role of Water Ice. The Astronomical Journal, 154.

Palomba, E., Compositional Differences among Bright Spots on the Ceres Surface, this issue.

Platz, T., et al. 2016. Surface Water-Ice Deposits in Northern Shadowed Regions of Ceres. Nature Astronomy 1, 0007.

Platz, T. et al. in press, Geological Mapping of the Ac-10 Rongo Quadrangle of Ceres, Icarus

Prettyman et al. 2016. Extensive Water ice within Ceres‘ aqueously altered regolith: Evidence from Nuclear Spectroscopy. Science, submitted.

Preusker, F. et al. 2016. Dawn at Ceres — Shape Model and Rotational State. Lunar Planet. Sci.XLVII, p.1954

Quick et al. A possible brine reservoir beneath Occator crater: thermal and compositional evolution and the formation of the Vinalia Faculae. This issue.

Raponi A. et al. Mineralogy of Occator Crater on Ceres. This issue.

Reddy, V.et al. 2012. Color and Albedo Heterogeneity of Vesta from Dawn. Science 336, Issue 6082, 700-704.

Reddy, V. 2015. Photometric Properties of Ceres from Telescopic Observations using Dawn Framing Camera Color Filters. Icarus 260, 332-345.

Ruesch et al. Bright Carbonate Surfaces on Ceres as Remnant of Salt-Rich Water Fountains, submitted to GRL

Russell, C. T., Raymond, C. A. 2012, The Dawn Mission to Minor Planets 4 Vesta and 1 Ceres (1st ed.; New York, Springer)

Russell, C. T.et al., 2016. Dawn arrives at Ceres:Exploration of a Small, Volatile-Rich World. Science 353. Issue 6303, 1008 - 1010.,

Schmedemann, N. 2016. Timing of optical maturation of recently exposed material on Ceres, Geophysical Research Letters, Volume 43, Issue 23, pp. 11.987-11.993.

Schmedemann, N. et al. 2017. The Distribution of Impact Ejecta on Ceres. Lunar Planet. Sci.XLVIII, 1233.

Schorghofer, N., Mazarico, E., Platz, T., Preusker, F., Schröder, S.E., Raymond, C.A., Russell, C.T. 2016. The permanently shadowed regions of dwarf planet Ceres. GRL 43, L069368.

Scully et al. The Formation and Evolution of Ceres' Occator Crater: introduction, geologic mapping and synthesis, this issue

Shepard M. K., Helfenstein, P. 2007. A Test of the Hapke Photometric Model. Journal of Geophysical Research, Volume 112, Issue E3.Sierks, H., et al. 2012. The Dawn Mission to Minor Planets 4 Vesta and 1 Ceres, ed. C.T. Russell et al. (New York, Springer), 263.

Sierks H. et al., 2011. The Dawn Framing Camera. Space Sci Rev. 163 (1–4), 263-327. Doi: 10.1007/s11214-011-9745-4.

Stein, N. et al.The Formation and Evolution of Bright Spots on Ceres. This issue.

Thangjam, G.; Hoffmann, M.; Nathues, A.; Li, J.-Y.; Platz, T. 2016. Haze at Occator Crater on Dwarf Planet Ceres, The Astrophysical Journal Letters, Volume 833, Issue 2, article id. L25, 9 pp.

Thangjam, G. et al. **in revision**, M&PS, Spectral properties and geology of bright and dark materials on dwarf planet Ceres

Torson, J. M., Becker, K. J. 1997. ISIS - A Software Architecture for Processing Planetary Images, Lunar Planet. Sci.XXVIII, p. 1443.

Travis, B.J, Bland P. A., Feldman W. C., Sykes M.V. 2015. Unconsolidated Ceres Model has a Warm Convecting Rocky Core and a Convecting Mud Ocean. , Lunar Planet. Sci.XLVI 2360.